Published in final edited form as:
Stem Cells. 2008 August ; 26(8): 2131–2141. doi:10.1634/stemcells.2008-0388.

G9a and Jhdm2a Regulate Embryonic Stem Cell Fusion-Induced Reprogramming of Adult Neural Stem Cells

Dengke K. Ma[a,b], **Cheng-Hsuan J. Chiang**[a,b], **Karthikeyan Ponnusamy**[a,c], **Guo-li Ming**[a,b,d], and **Hongjun Song**[a,b,d]

[a]Institute for Cell Engineering, Johns Hopkins University School of Medicine, Baltimore, Maryland, USA

[b]The Solomon H. Snyder Department of Neuroscience, Johns Hopkins University School of Medicine, Baltimore, Maryland, USA

[c]Department of Biomedical Engineering, Johns Hopkins University School of Medicine, Baltimore, Maryland, USA

[d]Department of Neurology, Johns Hopkins University School of Medicine, Baltimore, Maryland, USA

Abstract

Somatic nuclei can be reprogrammed to pluripotency through fusion with embryonic stem cells (ESCs). The underlying mechanism is largely unknown, primarily because of a lack of effective approaches to monitor and quantitatively analyze transient, early reprogramming events. The transcription factor Oct4 is expressed specifically in pluripotent stem cells, and its reactivation from somatic cell genome constitutes a hallmark for effective reprogramming. Here we developed a double fluorescent reporter system using engineered ESCs and adult neural stem cells/progenitors (NSCs) to simultaneously and independently monitor cell fusion and reprogramming-induced reactivation of transgenic Oct4-enhanced green fluorescent protein (EGFP) expression. We demonstrate that knockdown of a histone methyltransferase, G9a, or overexpression of a histone demethylase, Jhdm2a, promotes ESC fusion-induced Oct4-EGFP reactivation from adult NSCs. In addition, coexpression of Nanog and Jhdm2a further enhances the ESC-induced Oct4-EGFP reactivation. Interestingly, knockdown of G9a alone in adult NSCs leads to demethylation of the Oct4 promoter and partial reactivation of the endogenous Oct4 expression from adult NSCs. Our results suggest that ESC-induced reprogramming of somatic cells occurs with coordinated actions between erasure of somatic epigenome and transcriptional resetting to restore pluripotency. These mechanistic findings may guide more efficient reprogramming for future therapeutic applications of stem cells.

Correspondence: Hongjun Song, Ph.D., Institute for Cell Engineering, Department of Neurology, Johns Hopkins University School of Medicine, 733 North Broadway, BRB735, Baltimore, Maryland 21205, USA. Telephone: 443-287-7499; Fax: 410-614-9568; shongju1@jhmi.edu.

Author contributions: D.K.M., C.-H.J.C., and K.P.: conception and design, collection of data, data analysis, manuscript writing; G.-l.M., H.S.: conception and design, financial support, data analysis, manuscript writing.

Disclosure of Potential Conflicts of Interest
The authors indicate no potential conflicts of interest.

Keywords

Neural stem cells; Embryonic stem cells; Reprogramming; Oct4; Histone methyltransferase; Histone demethylase; G9a; Jhdm2a

Introduction

It is now established that highly differentiated somatic nuclei, of both mice and humans, can be converted into a pluripotent state by various methods, including somatic cell nuclear transfer (SCNT), ESC fusion-mediated reprogramming, and introducing defined genetic factors [1-7]. Accumulating evidence suggests that oocyte cytoplasm, ESCs and early embryos are enriched in reprogramming factors, which function to erase the somatic epigenome and re-establish a pluripotent signature of gene expression. However, the molecular identities of these reprogramming factors and the direct cellular mechanisms by which those factors work on somatic genomes remain incompletely understood. The transcription factor Nanog has been shown to promote the transfer of pluripotency after ESC fusion [8]. More recently, three or four transcription factors in combination have been shown to induce reprogramming of fibroblasts into an ESC-like state in culture [4 - 6]. Although these exciting advances have greatly facilitated efforts toward therapeutic cell reprogramming, the long-term nature of the methods and associated low efficiency raise important issues regarding the underlying mechanism. It is not known, for example, whether those transcription factors confer stable transcriptional circuits for pluripotency during long-term stringent culture conditions for ESCs or work in cooperation with other epigenetic regulators in early phases to actively induce reprogramming.

Oct4 encodes a member of the POU family of transcription factors that has been widely used as a specific marker for pluripotent ESCs [9, 10]. During early development, Oct4 is expressed mainly in the inner cell mass of blastocyst, and it becomes downregulated during cell differentiation. In somatic cells, Oct4 expression is repressed by epigenetic mechanisms involving both histone and DNA methylation to ensure silencing of Oct4 in a heritable manner [9, 11]. Consistent with its essential role for establishing pluripotency, both SCNT-mediated reprogramming and ESC-mediated reprogramming induce reactivation of Oct4 from somatic genomes [1, 12-14]. Interestingly, the extent of Oct4 reactivation is directly related to the developmental potential of somatic cell clones, and incomplete reactivation contributes to the low efficiency of somatic reprogramming [15]. Although the tight regulation of Oct4 attests to its utility as a reliable marker for successful reprogramming, specific mechanisms of how reprogramming activities induce genome-wide changes, including somatic Oct4 reactivation, remain to be identified.

Most of the current reprogramming regimes directly using ESCs typically involve polyethylene glycol (PEG)-induced cell fusion of ESCs and somatic cells carrying two different drug-resistant genes, followed by long-term selection to yield hybrid clones [1, 12, 14]. The low frequency of cell fusion makes it challenging to immediately identify cells that have undergone fusion. As a consequence, very little is known about the essential process of reprogramming at the early stage. Double drug selection also leads to massive cell death and

release of various factors, which may affect the reprogramming process. We sought to establish a novel method, which we termed Cre-LoxP-based, enhanced green fluorescent protein (EGFP) inducible assay for reprogramming (CLEAR). A combination of live fluorescent microscopy and quantitative flow cytometry allows for the monitoring of the early events during ESC fusion-induced reprogramming and quantitative analysis of the frequency and efficacy of reactivating Oct4-EGFP expression in adult somatic cells (Fig. 1A). Using CLEAR, we have identified a pair of opposing histone-modifying enzymes, the histone H3 lysine 9 (H3K9) methyltransferase G9a and the jumonji-domain containing H3K9 demethylase Jhdm2a [16-18], as epigenetic regulators for ESC fusion-induced Oct4-EGFP reactivation during reprogramming. Our study suggests that erasure of epigenetic methylation markers cooperates with transcriptional resetting to achieve pluripotency.

Materials and Methods

Constructs and Transfection

Turbo Cre cDNA was cloned into the MSCV retroviral vector that was modified to contain a puromycin-resistant gene under the control of IRES. pCAGT-bGeo-LoxP Cre excision reporter plasmid was made by cloning polymerase chain reaction (PCR)-amplified bGeo-LoxP fragments into pCAG-tdTomato/DsRed vectors. All clones were confirmed by sequencing. The JHDM2A-EGFP fusion construct was made by cloning CMV-EGFP (Clontech, Palo Alto, CA, http://www.clontech.com) fragments into the NdeI and KpnI sites of pcDNA3-hJHDM2a. Recombinant DNA research follows the National Institutes of Health guidelines. Transfections of ESCs, neural stem cells/progenitors (NSCs), and 293T cells were performed using Amaxa Nucleofection using programs (A-13 for ESCs, A-31 for NSCs and A-23 for 293T; Amaxa Inc., Gaithersburg, MD, http://www.amaxa.com) optimized to achieve high transfection efficiency and low toxicity.

Isolation and Establishment of Cre-Expressing NSC Lines

Adult NSCs were derived from either hippocampus or subventricular zone of 4–6-week-old Oct4-EGFP reporter mice. Specifically, dissected tissues were enzymatically dissociated. The cells were centrifuged at 200*g* for 5 minutes, resuspended in 0.9 M sucrose in 0.5× Hanks' balanced saline solution, and centrifuged for 10 minutes at 750*g*. The cell pellet was resuspended in 2 ml of culture medium, placed on top of 10 ml of 4% bovine serum albumin in EBSS solution, and centrifuged at 200*g* for 7 minutes, followed by washing in Dulbecco's modified Eagle's medium (DMEM)/Ham's F-12 medium (F12). Cells were plated onto plastic dishes in DMEM/F12 supplemented with N2, fibroblast growth factor 2 (20 ng/ml), heparin (5 μg/ml), and epidermal growth factor (20 ng/ml). NSC cultures were maintained in monolayer and passaged once they reached confluence. All animal procedures used in this study were performed in accordance with the protocol approved by the Institutional Animal Care and Use Committee at Johns Hopkins University School of Medicine.

An engineered retrovirus coexpressing Cre and the puromycin-resistant gene was produced and used for infection of NSCs as previously described [19, 20]. Briefly, retroviruses were produced through cotransfection of the vector and envelope plasmid VSVG in 293-GP packaging cells. Pools of supernatant were harvested and viruses were concentrated by

ultracentrifugation at 25,000 rpm for 1.5 hours. Aliquots of viruses were applied to proliferating NSC culture for 12–16 hours. NSCs were selected with 1 μg/ml puromycin for at least 1 week, and expanded resistant clones were verified for target gene expression using immunohistochemistry and Western blot analysis.

PEG-Induced Cell Fusion

The protocol was optimized for PEG-induced cell fusion between ESCs and NSCs to achieve maximum efficiency and minimal toxicity. Equal numbers of ESCs and NSCs were mixed thoroughly and spun down in phosphate-buffered saline. The pellet was loosened by gentle tapping, and 50% PEG (500 μl for 1×10^7 cells) was added to the cells continuously over 1 minute while the mixture was swirled at 37°C. Next, 2 ml of ESC medium was layered on top of PEG-cell mixture, followed by low-speed centrifugation at 1,800 rpm for 5 minutes. After the supernatant was removed, the cell pellet was incubated with ESC medium for 1 minute, washed, resuspended, and plated onto a gelatin-coated dish. Cells were cultured in Dulbecco's modified Eagle's medium, 15% fetal bovine serum supplemented with mouse leukemia inhibitory factor, 0.1 mM nonessential amino acids, 0.1 mM β-mercaptoethanol, and 50 U/ml penicillin/50 μg/ml streptomycin (ESC medium). Based on our CLEAR system, the cell fusion efficiency ($DsRed^+$ cell/total number of cells) is estimated to be 0.34% ± 0.06% under standard conditions. The following pharmacological inhibitors were applied in ESC-fusion experiments only during the first 48 hours after fusion: dimethyloxalylglycine (DMOG) (5–10 μM; BioMol), anacardic acid (5–10 μM; Calbiochem, San Diego, http://www.emdbiosciences.com), trichostatin A (TSA; 100 nM to 1 μM; Sigma-Aldrich, St. Louis, http://www.sigmaaldrich.com), and 5-aza-cytidine (1–5 μM; Sigma-Aldrich).

Microscopy and Flow Cytometry

Live images were taken from a Zeiss Axiovert 200M inverted microscope (Carl Zeiss, Jena, Germany, http://www.zeiss.com) through different optical filters. In dual-color flow cytometry, a FACSCalibur system (BD Biosciences, San Diego, http://www.bdbiosciences.com) was set up to ensure proper display of four parameters: forward scattering (FSC) and side scattering (SSC) as FL1 and 2, and green fluorescent protein (GFP) and DsRed as FL3 and FL4, respectively. Multiple control cells were used to set compensation for FL3 and FL4, followed by careful gate settings to isolate GFP^-DsRed^+ (R3), GFP^+DsRed^- (R2), and GFP^+DsRed^+ cell (R4) regions.

Immunocytochemistry

Cells were fixed with 4% paraformaldehyde, blocked in TBS++ (0.1 mM Tris-buffered saline, 5% donkey serum, 0.25% Triton X-100) for 1 hour, incubated with primary antibodies in TBS++ overnight at 4°C, and rinsed. The following primary antibodies were used: rabbit anti-H3K9me2 (1:500; Upstate, Charlottesville, VA, http://www.upstate.com), rabbit anti-GFP (1:500; Molecular Probes, Eugene, OR, http://probes.invitrogen.com), mouse monoclonal anti-Cre (1:1,000; Sigma-Aldrich), rabbit anti-DsRed (1:1,000; Clontech), mouse monoclonal anti-Oct4 (1:100; Santa Cruz Biotechnology Inc., Santa Cruz, CA, http://www.scbt.com), and mouse or rabbit IgG isotype control (Santa Cruz

Biotechnology). After incubation with fluorophore-conjugated secondary antibodies (1:250; Jackson Immunoresearch) for 90 minutes at room temperature, cells were stained with 4′,6-diamidino-2-phenylindole, mounted, and stored at 4°C. Images were taken with a confocal microscopy system (Zeiss LSM510).

Short Hairpin RNA-Mediated Knockdown and Real-Time PCR

The following short hairpin sequences were cloned into retroviral vector pUEG: TGAGAGAGGATGATTCTTA (short hairpin RNA [shRNA]-G9a) and TTCTCCGAACGTGTCACGT (shRNA-nonsilencing control). Efficiency of the shRNAs in NSCs was confirmed by real-time quantitative (qRT) PCR.

For qRT-PCR, total RNA was extracted using an RNeasy kit (Qiagen, Hilden, Germany, http://www1.qiagen.com) and converted to cDNA by SuperScript III (Invitrogen, Carlsbad, CA, http://www.invitrogen.com). cDNA samples were added to a SYBR Green-based quantitative PCR mixture and analyzed using the ddCt methods. *β*-Actin served as an internal control for normalization. The following primers for G9a, Jhdm2a, Oct4, and *β*-Actin were used: CAACTTCCAGAGCGACCAG (G9a forward), ACCTCCAGGTGGTTGTTCAC (G9a reverse), GAAGGCTTCTTAACACCAAACAA (Jhdm2a forward), CATTTGACAGAAGTGGTCTCCA (Jhdm2a reverse), CAGAAGGGCAAAAGATCAAGTAT (Oct4 reverse), CAGTTTGAATGCATGGGAGA (Oct4 forward), TCAACACCCCAGCCATGTA (Actin forward), and CAGGTCCAGACGCAGGAT (Actin reverse).

Bisulfite Genomic Sequencing

For bisulfite genomic sequencing, 500 ng of genomic DNA from each sample was digested by EcoRI overnight, followed by boiling for 5 minutes and incubation in 0.3 M NaOH at 50°C for 15 minutes. Denatured DNA was then embedded in 0.67% (wt/vol) low-melting point agarose beads and treated with a mixture of 2.5 M sodium bisulfite, 0.4 M NaOH, and 0.13 M hydroquinone at 50°C overnight. Beads were then washed with TE buffer and treated with 0.2 M NaOH for 30 minutes, followed by washing with TE buffer for 30 minutes. Prior to PCR amplification, beads were washed with H_2O for 30 minutes. Fresh PCR products were cloned by the TA cloning method and sequenced. Efficiency of bisulfite conversion was monitored by the presence of unconverted C residues in non-CpG regions, which were only seldom seen. The primers used for the Oct4 promoter and enhancer region (Fig. 7A) were TGGGTTGAAATATTGGGTTTATTT and CTAAAACCAAATATCCAACCATA. These primers were designed to span part of the Oct4 coding region and thus directly reflect the endogenous promoter status.

Results

Visualization of ESC Fusion-Induced Oct4 Reactivation in Adult NSCs with CLEAR

The CLEAR strategy uses engineered ESCs and NSCs to monitor fusion-induced DsRed expression and reprogramming-induced EGFP expression (Fig. 1A). Z-Red ESCs were derived from a clonal ESC line containing one copy of a transgene (CAG-loxP-LacZ::neomycin-polyA-loxP-DsRed. T3) that serves as a Cre recombination excision

reporter [21]. Upon introduction of Cre activity, transfected cells exhibited strong red fluorescence resulting from the DsRed expression (supplemental online Fig. 1A). This line of ESCs has previously been used to generate reporter mice [21], and we confirmed that Z-Red ESCs were capable of reprogramming somatic NSCs after fusion followed by long-term double drug selection (supplemental online Fig. 2).

Adult NSCs were isolated from Oct4-EGFP (GOF18-ΔPE-EGFP) transgenic mice [22, 23] and transduced by retroviruses to stably coexpress Cre and the puromycin resistance gene through a bicistronic cassette (hereafter termed CIPOE NSCs). Somatic cells with Oct4-GFP transgene integration have been used previously to investigate reprogramming, in which the regulatory elements of Oct4 direct reliable GFP reactivation from somatic genomes in reprogrammed ESC-like hybrid cells [12, 14] (also described in supplemental online Fig. 2). Multiple CIPOE NSC lines from Oct4-EGFP transgenic mice were established, characterized, and used for subsequent cell fusion experiments. Functional Cre activity was demonstrated by the strong nuclear Cre immunoreactivity and effective excision of the LoxP-flanking element after transfection with a reporter plasmid (supplemental online Fig. 1B).

We first examined the temporal and spatial resolution of the CLEAR strategy by monitoring cell fusion and reprogramming-induced Oct4-EGFP expression. PEG 1500 was used to induce cell fusion since the spontaneous fusion rate is extremely low under normal conditions without any selection pressure (data not shown). After induced fusion between Z-Red ESCs and CIPOE NSCs, we observed the emergence of $DsRed^+$ cells at 24 and 48 hours (Fig. 1B), suggesting that Cre-mediated recombination and subsequent DsRed expression occurred rapidly and allowed early identification of potential reprogramming events in fused cells. Interestingly, although many $DsRed^+$ cells remained GFP^-, some GFP^+ cells were observed at 48 hours, indicating that ESC-induced reactivation of Oct4 expression was initiated. At 96 hours after fusion, the majority of $DsRed^+$ cells were GFP^+ (Fig. 1C), suggesting that ESC fusion-induced reactivation of Oct4 expression from somatic cells is highly efficient. We also noted that the GFP^+ cells tended to appear first from the outlining boarder of a colony (Fig. 1B), implying a spatial order and variegated speed of reprogramming among the fused cell population. These results showed that CLEAR is capable of visualizing the early fused cells and reprogramming-induced Oct4-EGFP reactivation simultaneously and yields both temporal and spatial information on reprogramming.

Characterization of ESC Fusion-Induced Reprogramming with CLEAR

To quantitatively analyze reprogramming-induced Oct4-EGFP reactivation, we used dual-color flow cytometry to display and measure the cell population that underwent PEG-induced cell fusion. Viable cells were identified by their typical FSC and SSC properties. To ensure appropriate gating for GFP^+ and $DsRed^+$ events and to compensate the spectrum overlap of GFP and DsRed signals, we first calibrated the system using multiple control cells, including Z-Red ESCs, CIPOE NSCs, mixed Z-Red ESCs and CIPOE NSCs without PEG, Z-Red ESCs transfected with a constitutive Cre expression plasmid, and CIPOE NSCs transfected with a Cre excision reporter plasmid (Fig. 2A). The resulting gates allowed us to

accurately quantify $DsRed^{+}GFP^{+}$ cells and $DsRed^{+}GFP^{-}$ cells, as shown in typical analytic dot plots (Fig. 2A).

We quantitatively measured ESC fusion-induced Oct4 reactivation from NSCs using two different approaches. First, reprogramming frequency was determined by the ratio of $GFP^{+}DsRed^{+}$ cells to total $DsRed^{+}$ cells. Time course analysis showed that over a period of the initial 8 days after fusion, the reprogramming frequency increased from 20% ± 5% at day 2 to 90% ± 2% at day 8 ($n = 4$; Fig. 2B). The spontaneous reprogramming frequency in the absence of PEG was below the detection threshold. Second, reprogramming efficacy was examined by plotting the distribution of GFP fluorescence intensities of individual cells from the $DsRed^{+}$ population (Fig. 2C). This analysis provided a measurement of the efficiency of Oct4-EGFP reactivation in NSCs after successful fusion. We found that reprogramming efficacy steadily increased up to 8 days after induction of fusion (Fig. 2C). In contrast, fusion-induced DsRed expression did not change significantly during days 2 and 8 (supplemental online Fig. 3A). With these two types of analysis, our CLEAR strategy enables quantification of the reprogramming frequency and efficacy over time, especially at critical early stages after cell fusion.

Involvement of Chromatin Demethylation in ESC-Induced Oct4 Reactivation in Adult Somatic Stem Cells

To explore the underlying mechanism for reprogramming, we first assessed the potential involvement of chromatin-modifying enzymes. We screened a panel of pharmacological inhibitors of histone acetyltransferases, deacetylases, methyltransferases, and demethylases during the first 48 hours after fusion. Administration of inhibitors only during the early time window after fusion ensures specific effects on reprogramming but not long-term nonspecific effects on survival, proliferation, and differentiation of hybrid cells. We found that the HDAC inhibitor TSA and various other inhibitors either were ineffective, were toxic to the cells, or led to mild deficit in reprogramming-induced Oct4 reactivation (supplemental online Table 1). In contrast, DMOG, an inhibitor of Fe^{2+}- and 2-oxoglutarate-dependent dioxygenases [24, 25], including the AlkB family of DNA repair demethylases and the jumonji family of histone demethylases [26-28], significantly reduced ESC-induced Oct4 reactivation in NSCs. To confirm the blocking effects of DMOG on histone demethylases, we used an immunolabeling assay previously developed for JHDM2A. Overexpression of Jhdm2a in heterologous cell lines led to dramatic loss of H3K9 dimethylation, which was clearly blocked by DMOG treatment (10 μM; Fig. 3A). CLEAR analysis showed that treatment with DMOG, but not dimethyl sulfoxide (DMSO), resulted in significant decreases in both reprogramming frequency and efficacy (Fig. 3B-3D). In contrast, Cre-mediated DsRed expression remained unchanged compared with control DMSO treatment (supplemental online Fig. 3B). These experiments indicate that activities of dioxygenases, including chromatin-associated histone demethylases or putative DNA demethylases, are likely essential for ESC-induced reprogramming of the adult NSCs.

Regulation of ESC-Induced Oct4 Reactivation in Adult NSCs by G9a and Jhdm2a

We next examined molecular identities of epigenetic factors that play critical roles in reprogramming. Previous studies suggest that in somatic cells, H3K9 methylation near the

Oct4 promoter region is mediated by enchromatin-specific histone methyltransferase G9a [16]. We found that G9a expression is significantly higher in the somatic CIPOE cells than in ESCs (Fig. 4A). Since ESC-induced reactivation of Oct4 is accompanied by histone and DNA demethylation during reprogramming, we examined whether H3K9-specific methyltransferase G9a may antagonize reprogramming. Using a previously validated shRNA for mouse G9a [29], we were able to significantly knock down expression of endogenous G9a in CIPOE cells, as shown by quantitative real-time PCR (Fig. 4A). Interestingly, expression of shRNA-G9a, but not the control shRNA, in stable lines of CIPOE NSCs accelerated the speed of ESC-induced Oct4-EGFP expression, as shown by 110% and 26% increases in the reprogramming frequency at days 2 and 4, respectively (Fig. 4C). The efficacy of ESC-induced Oct4-EGFP reactivation in NSCs was also significantly enhanced at days 2 and 4 (Fig. 4C). These results suggest that H3K9 methyltransferase G9a constrains ESC-induced Oct4 reactivation during early phases of reprogramming in somatic cells.

Dynamic histone methylation may result from opposing actions of histone methyltransferases and demethylases [26]. Given our preliminary findings from pharmacological analysis (Fig. 3), we next sought to identify the histone demethylase that may promote the reprogramming process. We surveyed expression of known histone demethylases through expressed sequence tag counts at different developmental stages in various tissues. We found that Jhdm2a is highly expressed in the early mouse embryo and is particularly abundant in the ovum, which is known to be enriched in reprogramming activities (Fig. 5A). Further analysis with quantitative real-time PCR showed that the expression level of Jhdm2a was four times higher in ESCs than that in adult NSCs (Fig. 5B). To examine a potential role of Jhdm2a in reprogramming, we overexpressed Jhdm2a in CIPOE NSCs and confirmed that overexpression of Jhdm2a, but not of an enzymatically inactive mutant (Jhdm2a-H1120Y), induced genome-wide loss of H3K9 dimethylation (Fig. 5C). CLEAR analysis showed that overexpression of wild-type Jhdm2a in CIPOE NSCs increased the frequency of ESC-induced Oct4-EGFP reactivation by 36% at day 4, but not at day 2 as in the case of G9a knockdown (Fig. 5D). The efficacy of ESC-induced Oct4-EGFP reactivation was also significantly enhanced at day 4 (Fig. 5E). In contrast, overexpression of the mutant Jhdm2a (H1120Y) exhibited no detectable effects on reprogramming frequency and efficacy (Fig. 5D, 5E), indicating that the catalytic H3K9 demethylation activity of Jhdm2a is important for promoting ESC-induced reactivation of Oct4-EGFP expression in adult NSCs. Taken together, these results suggest that H3K9 (de)methylation mediated by the coordinated actions between Jhdm2a and G9a regulates ESC-induced reactivation of Oct4-EGFP expression in adult NSCs.

Nanog Enhances Effects of Jhdm2a on Oct4 Reactivation in Somatic Stem Cells

Previous studies have shown that long-term expression of the pluripotency gene Nanog promotes ESC fusion-induced reprogramming and suggested that Nanog may collaborate with unknown epigenetic regulators to facilitate reprogramming [8] (Fig. 6A). CLEAR analysis showed that overexpression of Nanog in CIPOE NSCs substantially increased the reprogramming frequency at day 4 (Fig. 6B). The reprogramming efficacy was also significantly enhanced with Nanog overexpression at day 4 (Fig. 6C). These results suggest

that short-term Nanog overexpression accelerates ESC-induced Oct4-GFP reactivation in adult somatic cells and are consistent with previous findings on long-term effects of Nanog expression [8].

To test whether Jhdm2a-mediated H3K9 demethylation constitutes one of the epigenetic modification activities in coordination with the action of ESC-specific transcription factors (Fig. 6A), we coexpressed both Jhdma2a and Nanog in CIPOE NSCs and examined the reprogramming on the basis of CLEAR analysis. Interestingly, such combination led to further enhancement of reprogramming frequency and efficacy in a time window ranging from day 2 to day 6 (Fig. 6B, 6C).

DNA Demethylation of the Oct4 Promoter and Partial Reactivation of Endogenous Oct4 Expression by G9a Knockdown in Adult NSCs

Successful reprogramming requires erasure of the somatic epigenome, including both histone and DNA modifications [13, 30, 31]. We tested whether DNA demethylation of the pluripotency gene *Oct4* may partially account for the facilitating effects of histone demethylation during ESC fusion-induced reprogramming. Extensive bisulfite sequencing revealed that ESC fusion dramatically reduced DNA methylation in Oct4 promoter regions compared with that in CIPOE NSCs (Fig. 7A). Surprisingly, independently of cell fusion, CIPOE NSCs expressing shRNA against G9a, but not a control shRNA, exhibited significantly decreased DNA methylation in Oct4 promoter regions, with levels very similar to those in Z-Red ESCs or reprogrammed hybrid clones (Fig. 7A). Since bisulfite sequencing primers were designed to span part of the Oct4 coding region, the observed demethylation reflects the endogenous promoter status. We also evaluated the impact of G9a knockdown on endogenous Oct4 expression. Interestingly, the expression of endogenous Oct4 became partially reactivated in adult NSCs expressing shRNA against G9a, as shown by both conventional (Fig. 7B) and quantitative (Fig. 7C) PCR. The mRNA level of Oct4 measured in bulk adult NSC cultures with G9a knockingdown reached approximately 10% of that in ESCs, whereas little expression was detected in CIPOE cells alone or CIPOE cells expressing the control shRNA. Taken together, these results suggest that G9a is critical to impose epigenetic silencing machinery on Oct4 by maintaining DNA methylation in adult NSCs. Removing G9a induces either active or passive DNA demethylation [32-34] that relieves the epigenetic silencing and facilitates ESC-induced reprogramming of somatic cells.

Discussion

Rapid advances in stem cell biology have created fascinating possibilities to reprogram somatic nuclei for therapeutic applications [3, 35]. Mechanistic understanding of reprogramming will likely benefit from studies using a variety of reprogramming paradigms, including SCNT, cell fusion, purified protein extracts, and genetic manipulation using defined factors. Based on the cell fusion paradigm, CLEAR enables direct and independent visualization of rare fusion and transient reprogramming events at a single cell level. Such a sensitive method allows quantitative analysis of ESC fusion-induced Oct4 reactivation during initial stages of reprogramming of adult somatic stem cells, especially the temporal

regulation. Using Oct-4 reactivation as a readout of reprogramming, we observed that cell fusion does not necessarily guarantee reprogramming, and on average it takes at least 4 days for reprogramming to complete. Furthermore, the reprogramming speed is heterogeneous within an ESC-like fusion colony. CLEAR also uses the analytic power of dual-color flow cytometry for quantification of both reprogramming frequency and efficacy. We noted that cell fusion also induced a small subset of GFP^+ but $DsRed^-$ cells, possibly caused by inefficient recombination due to heterogeneous levels of Cre expression. Nevertheless, the accurate analysis of Oct4 reactivation was not compromised in this study, since only successfully fused $DsRed^+$ cells were taken into consideration. Importantly, the reprogramming efficacy of $DsRed^+$ cells is representative of the total cell population (supplemental online Fig. 3C).

The remarkable reversibility of cellular differentiation was first demonstrated in amphibian cells and has recently been demonstrated in mammalian cells [2, 3, 36]. These SCNT experiments suggest that the somatic epigenome requires extensive reprogramming to achieve toti- or pluripotency. However, there is increasing evidence that epigenetic reprogramming is heterogeneous and severely deficient in some cloned embryos. Indeed, it has been shown that H3K9 and associated DNA hypermethylation are closely correlated with restricted developmental potential in cloned embryos [15]. Corroborating these studies, here we show that H3K9 and DNA methylation restricts somatic cell reprogramming by ESCs. Taken together, these results underscore the crucial role of dynamic demethylation in determining reprogramming efficacy by both SCNT and fusion-induced paradigms. By overexpression of Jhdm2a, we observed genome-wide H3K9 demethylation, and in parallel, knockdown of G9a induced DNA demethylation at the Oct4 promoter. These epigenetic erasure activities may represent a critical initial process of reprogramming, which is coupled with re-establishment of pluripotency-specific transcriptional programs mediated by a cohort of transcriptional factors, such as Nanog (Fig. 6A).

Recent exciting advances using candidate approaches have identified defined factors that are sufficient to reprogram adult somatic cells into pluripotent ESC-like cells with an epigenome highly similar to that of normal ESCs [4 - 6, 37, 38]. Because reprogramming using these defined factors is achieved through long-term cell growth in culture and with low efficiency, mechanisms underlying reprogramming largely remain a black box. Complementary to studies on these defined factors, we show that ESC fusion-induced Oct4 reactivation occurs within a rather short period of time (2–4 days) and at high efficiency (up to 95% of all fused cells). In addition, our results suggest that the early phase of reprogramming may critically involve extensive epigenetic remodeling and that transcription factors may play long-term roles in both recruiting epigenetic regulators and stabilizing the pluripotent epigenome (Fig. 6A).

Although previous studies have shown that Oct4-EGFP or endogenous Oct4 reactivation accurately reflects the effectiveness of reprogramming [1, 12, 14], additional studies are necessary to test whether the specific mechanisms we have identified also operate for reactivation of other pluripotency-specific genes. Importantly, the Oct4 transgenic promoter in our CLEAR system includes the distal enhancer without the proximal enhancer, which ensures a highly specific and appropriate level of Oct-4 expression in undifferentiated

pluripotent tissue to be reported. It has been shown that Jhdm2a regulates ESC self-renewal, whereas G9a plays critical roles in silencing Oct4 during differentiation of ESCs, and differentiating $G9a^{-/-}$ ESCs have a higher probability to revert back to an initial ESC state [16, 39]. Our bisulfite sequencing analysis suggests that G9a may be directly associated with DNA methylation of the Oct4 promoter, although the full activation of the promoter may depend on pluripotency-specific transcription factors. Nevertheless, effects of G9a and Jhdma2a on ESC fusion-induced reprogramming are distinct compared with that of Nanog, especially during the initial days of reprogramming (Figs. 4B, 5D, 6B), highlighting the relative importance of epigenetic and genetic regulation in early phases of reprogramming. Considering that H3K9 dimethylation constitutes only one of many histone modifications, it is likely that other histone demethylases or methyltransferases may also be critically involved in regulation of reprogramming.

Summary

DNA and histone modification-mediated epigenetic reprogramming has long been postulated to be essential at stages when developmental potency of cells changes, such as during SCNT and fusion with ESCs, yet experimental evidence for the role of specific enzymes is scant. Using the newly developed quantitative system CLEAR, we have identified a pair of histone-modifying enzymes, G9a and Jhdm2a, as epigenetic regulators for Oct4-EGFP reactivation during ESC-induced reprogramming. Our mechanistic findings may explain the low efficiency of currently adopted reprogramming regimes and may therefore guide more efficient reprogramming using defined factors or chemicals in the near future. For example, a recent chemical screen has identified a biologically active G9a inhibitor that may be useful in reprogramming somatic cells [40]. More broadly, the CLEAR system may aid the identification of additional reprogramming factors [7], facilitate our molecular understanding of how a somatic genome can be reprogrammed, and ultimately advance efforts to engineer the developmental potential of somatic cells for therapeutic applications.

Supplementary Material

Refer to Web version on PubMed Central for supplementary material.

Acknowledgments

We thank K.A. Sixt, A. Venkatesan, and M. Bonaguidi for comments and suggestions; L.-h. Liu for technical support; X. Yu and L. Cheng for help on flow cytometry; A. Nagy for Z-Red ESCs; P. Donovan for Oct4-EGFP transgenic mice; and Y. Zhang, T. Rotolo, J. Nathans, S. Kim, and V. Dawson for reagents and assistance. This work was supported by NIH Grants NS047344 and AG024984, the Packard Center for ALS and Muscular Dystrophy Association, a McKnight Scholar Award, and the Maryland Stem Cell Research Fund (to H.S.) and by NIH Grant NS048271, the Adelson Medical Research Foundation, The Klingenstein Award in the Neuroscience, the March of Dimes, and the Maryland Stem Cell Research Fund (to G.-l.M.). D.K.M. was a predoctoral fellow of the American Heart Association. C.-H.J.C. was supported by a Taiwan Merit Scholarship.

References

1. Cowan CA, Atienza J, Melton DA, et al. Nuclear reprogramming of somatic cells after fusion with human embryonic stem cells. Science. 2005; 309:1369–1373. [PubMed: 16123299]

2. Gurdon JB. From nuclear transfer to nuclear reprogramming: The reversal of cell differentiation. Annu Rev Cell Dev Biol. 2006; 22:1–22. [PubMed: 16704337]
3. Hochedlinger K, Jaenisch R. Nuclear reprogramming and pluripotency. Nature. 2006; 441:1061–1067. [PubMed: 16810240]
4. Yu J, Vodyanik MA, Smuga-Otto K, et al. Induced pluripotent stem cell lines derived from human somatic cells. Science. 2007; 318:1917–1920. [PubMed: 18029452]
5. Takahashi K, Yamanaka S. Induction of pluripotent stem cells from mouse embryonic and adult fibroblast cultures by defined factors. Cell. 2006; 126:663–676. [PubMed: 16904174]
6. Park IH, Zhao R, West JA, et al. Reprogramming of human somatic cells to pluripotency with defined factors. Nature. 2008; 451:141–146. [PubMed: 18157115]
7. Wong CC, Gaspar-Maia A, Ramalho-Santos M, et al. High-efficiency stem cell fusion-mediated assay reveals Sall4 as an enhancer of reprogramming. PLoS ONE. 2008; 3:e1955. [PubMed: 18414659]
8. Silva J, Chambers I, Pollard S, et al. Nanog promotes transfer of pluripotency after cell fusion. Nature. 2006; 441:997–1001. [PubMed: 16791199]
9. Pesce M, Scholer HR. Oct-4: Gatekeeper in the beginnings of mammalian development. Stem Cells. 2001; 19:271–278. [PubMed: 11463946]
10. Pan GJ, Chang ZY, Scholer HR, et al. Stem cell pluripotency and transcription factor Oct4. Cell Res. 2002; 12:321–329. [PubMed: 12528890]
11. Hattori N, Nishino K, Ko YG, et al. Epigenetic control of mouse Oct-4 gene expression in embryonic stem cells and trophoblast stem cells. J Biol Chem. 2004; 279:17063–17069. [PubMed: 14761969]
12. Do JT, Scholer HR. Nuclei of embryonic stem cells reprogram somatic cells. Stem Cells. 2004; 22:941–949. [PubMed: 15536185]
13. Simonsson SGJ. DNA demethylation is necessary for the epigenetic reprogramming of somatic cell nuclei. Nat Cell Biol. 2004; 6:10.
14. Tada M, Takahama Y, Abe K, et al. Nuclear reprogramming of somatic cells by in vitro hybridization with ES cells. Curr Biol. 2001; 11:1553–1558. [PubMed: 11591326]
15. Santos F, Zakhartchenko V, Stojkovic M, et al. Epigenetic marking correlates with developmental potential in cloned bovine preimplantation embryos. Curr Biol. 2003; 13:1116–1121. [PubMed: 12842010]
16. Feldman N, Gerson A, Fang J, et al. G9a-mediated irreversible epigenetic inactivation of Oct-3/4 during early embryogenesis. Nat Cell Biol. 2006; 8:188–194. [PubMed: 16415856]
17. Tachibana M, Sugimoto K, Nozaki M, et al. G9a histone methyltransferase plays a dominant role in euchromatic histone H3 lysine 9 methylation and is essential for early embryogenesis. Genes Dev. 2002; 16:1779–1791. [PubMed: 12130538]
18. Yamane K, Toumazou C, Tsukada Y, et al. JHDM2A, a JmjC-containing H3K9 demethylase, facilitates transcription activation by androgen receptor. Cell. 2006; 125:483–495. [PubMed: 16603237]
19. Ge S, Goh EL, Sailor KA, et al. GABA regulates synaptic integration of newly generated neurons in the adult brain. Nature. 2006; 439:589–593. [PubMed: 16341203]
20. Duan X, Chang JH, Ge S, et al. Disrupted-In-Schizophrenia 1 regulates integration of newly generated neurons in the adult brain. Cell. 2007; 130:1146–1158. [PubMed: 17825401]
21. Vintersten K, Monetti C, Gertsenstein M, et al. Mouse in red: Red fluorescent protein expression in mouse ES cells, embryos, and adult animals. Genesis. 2004; 40:241–246. [PubMed: 15593332]
22. Song H, Stevens CF, Gage FH. Astroglia induce neurogenesis from adult neural stem cells. Nature. 2002; 417:39–44. [PubMed: 11986659]
23. Yeom YI, Fuhrmann G, Ovitt CE, et al. Germline regulatory element of Oct-4 specific for the totipotent cycle of embryonal cells. Development. 1996; 122:881–894. [PubMed: 8631266]
24. Hausinger RP. FeII/alpha-ketoglutarate-dependent hydroxylases and related enzymes. Crit Rev Biochem Mol Biol. 2004; 39:21–68. [PubMed: 15121720]
25. Chen H, Ke Q, Kluz T, et al. Nickel ions increase histone H3 lysine 9 dimethylation and induce transgene silencing. Mol Cell Biol. 2006; 26:3728–3737. [PubMed: 16648469]

26. Klose RJ, Zhang Y. Regulation of histone methylation by demethylimination and demethylation. Nat Rev Mol Cell Biol. 2007; 8:307–318. [PubMed: 17342184]
27. Falnes PO, Klungland A, Alseth I, et al. Repair of methyl lesions in DNA and RNA by oxidative demethylation. Neuroscience. 2007; 145:1222–1232. [PubMed: 17175108]
28. Sedgwick B. Repairing DNA-methylation damage. Nat Rev Mol Cell Biol. 2004; 5:148–157. [PubMed: 15040447]
29. Lee DY, Northrop JP, Kuo MH, et al. Histone H3 lysine 9 methyltransferase G9a is a transcriptional coactivator for nuclear receptors. J Biol Chem. 2006; 281:8476–8485. [PubMed: 16461774]
30. Jenuwein T, Allis CD. Translating the histone code. Science. 2001; 293:1074–1080. [PubMed: 11498575]
31. Kimura H, Tada M, Nakatsuji N, et al. Histone code modifications on pluripotential nuclei of reprogrammed somatic cells. Mol Cell Biol. 2004; 24:5710–5720. [PubMed: 15216876]
32. Bird A. Perceptions of epigenetics. Nature. 2007; 447:396–398. [PubMed: 17522671]
33. Barreto G, Schafer A, Marhold J, et al. Gadd45a promotes epigenetic gene activation by repair-mediated DNA demethylation. Nature. 2007; 445:671–675. [PubMed: 17268471]
34. Estève PO, Chin HG, Smallwood A, et al. Direct interaction between DNMT1 and G9a coordinates DNA and histone methylation during replication. Genes Dev. 2006; 20:3089–3103. [PubMed: 17085482]
35. Pomerantz J, Blau HM. Nuclear reprogramming: A key to stem cell function in regenerative medicine. Nat Cell Biol. 2004; 6:810–816. [PubMed: 15340448]
36. Gurdon JB, Elsdale TR, Fischberg M, et al. Sexually mature individuals of Xenopus laevis from the transplantation of single somatic nuclei. Nature. 1958; 182:64–65. [PubMed: 13566187]
37. Maherali RS, Xie W, Utikal J, et al. Directly reprogrammed fibroblasts show global epigenetic remodeling and widespread tissue contribution. Cell Stem Cell. 2007; 1:55–70. [PubMed: 18371336]
38. Wernig M, Meissner A, Foreman R, et al. In vitro reprogramming of fibroblasts into a pluripotent ES-cell-like state. Nature. 2007; 448:318–324. [PubMed: 17554336]
39. Loh YH, Zhang W, Chen X, et al. Jmjd1a and Jmjd2c histone H3 Lys 9 demethylases regulate self-renewal in embryonic stem cells. Genes Dev. 2007; 21:2545–2557. [PubMed: 17938240]
40. Kubicek S, O'Sullivan RJ, August EM, et al. Reversal of H3K9me2 by a small-molecule inhibitor for the G9a histone methyltransferase. Mol Cell. 2007; 25:473–481. [PubMed: 17289593]

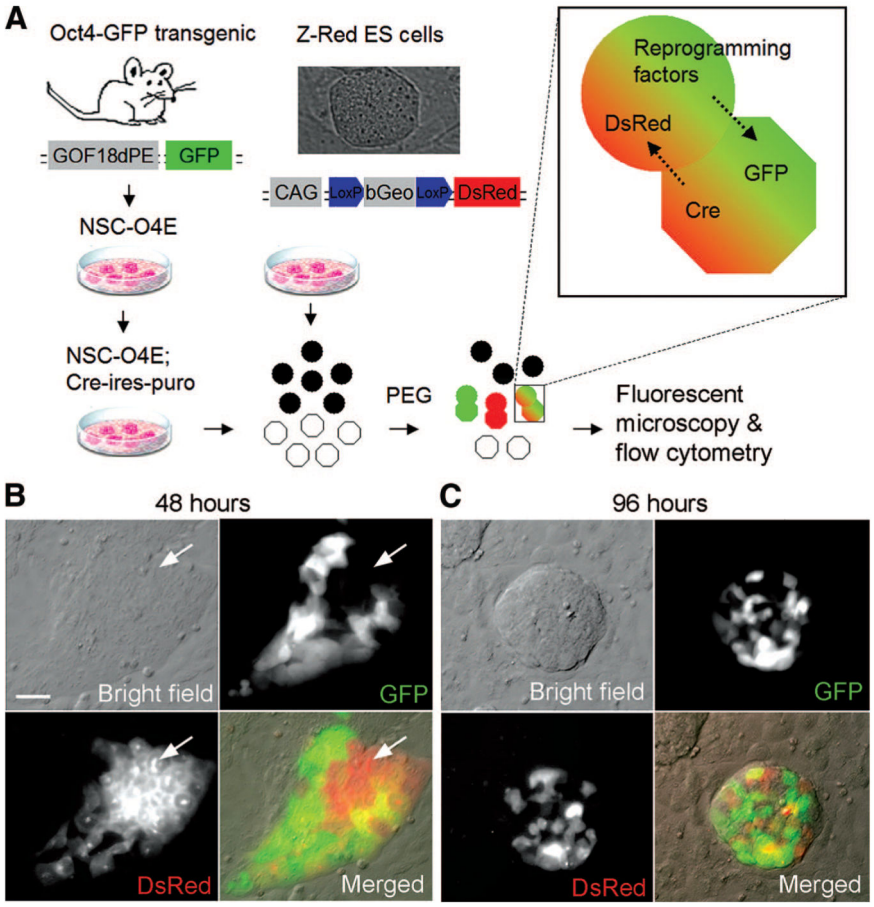

Figure 1.

Cre-loxP-based, enhanced green fluorescent protein-inducible assay for reprogramming (CLEAR). **(A):** A diagrammatic illustration of CLEAR analysis. CIPOE NSC lines were established by infection of adult NSCs derived from transgenic mice harboring Oct4-enhanced green fluorescent protein reporter with retroviruses to coexpress the Cre recombinase and puromycin resistance gene. Z-Red ESCs carry an inducible DsRed expression cassette upon Cre-mediated excision. PEG-induced fusion of Z-Red ESCs and CIPOE NSCs leads to GFP expression as an indicator of Oct4 reactivation and DsRed expression as a reporter for fusion events. The dual-color reporter system can be monitored by both live fluorescence microscopy and quantitative flow cytometry to probe reprogramming processes. **(B, C):** Live images of fused ES-like colonies. Shown are sample images of fused ES-like colonies at 48 hours **(B)** and 96 hours **(C)** after PEG-induced fusion between CIPOE NSCs and Z-Red ESCs. Arrows point to $DsRed^{+}GFP^{-}$ cells that were successfully fused but incompletely reprogrammed. Scale bar = 20 μm. Abbreviations: ES, embryonic stem; GFP, green fluorescent protein; ires, internal ribosome entry site; NSC, neural stem cell/progenitor; O4E, Oct4-enhanced green fluorescent protein; PEG, polyethylene glycol.

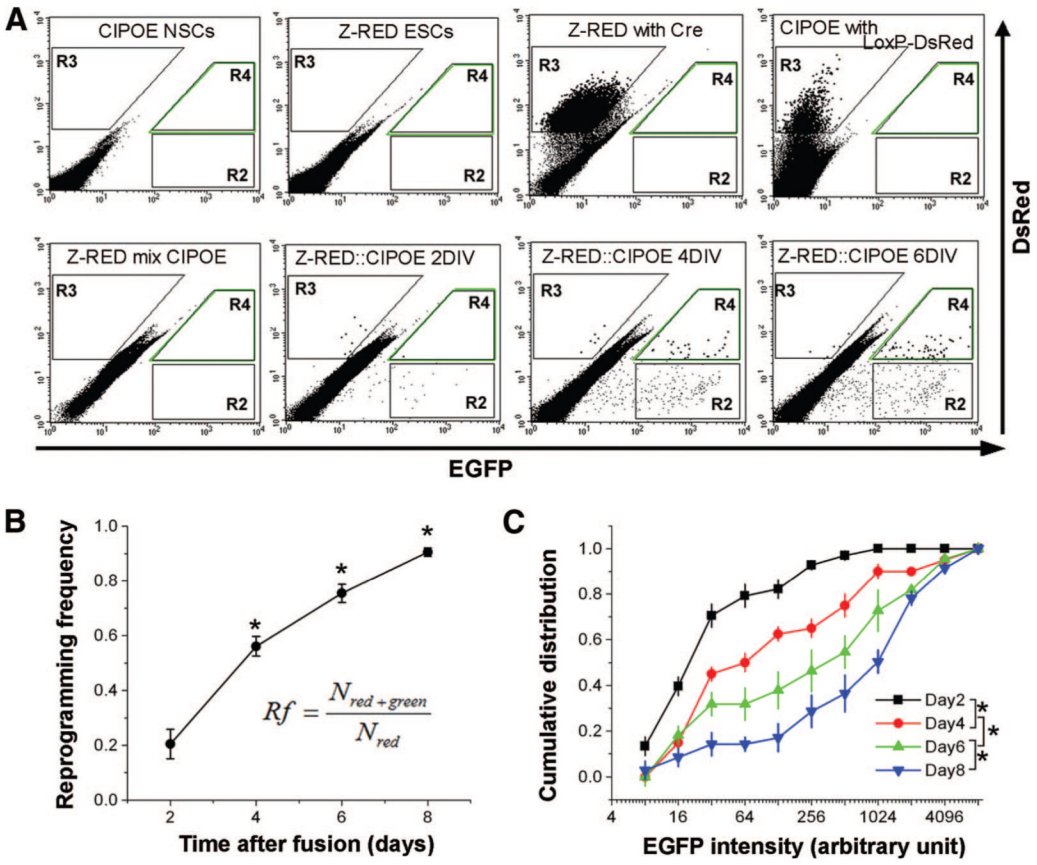

Figure 2.

Flow cytometry analysis of Oct4-EGFP reactivation using Cre-loxP-based, enhanced green fluorescent protein-inducible assay for reprogramming. **(A):** Representative dot plots. Shown are sample plots from a control cell population including CIPOE NSCs only; Z-Red ESCs only; Z-Red ESCs transfected with a constitutive Cre expression plasmid; CIPOE NSCs transfected with a Cre reporter plasmid (pCAGT-bGeo-LoxP) and a mix of Z-Red ESCs without polyethylene glycol (PEG); and from PEG-induced fusion cell population at 2, 4, and 6 DIV. **(B):** Analysis of Rf. Rf was calculated from multiple independent experiments and quantified for fusion population over 2, 4, 6, and 8 days after PEG treatment. Values represent mean ± SEM ($n = 5$; *, $p < .01$, one-way analysis of variance). **(C):** Analysis of reprogramming efficacy. Shown is the summary of cumulative distribution plot of EGFP intensity for grouped DsRed$^+$ cells over 2, 4, 6, and 8 days after PEG treatment. Values represent mean ± SEM ($n = 5$; *, $p < .01$, Kolmogorov-Smirnov test). Abbreviations: DIV, days in vitro; EGFP, enhanced green fluorescent protein; mix, mixture; NSC, neural stem cell/progenitor; Rf, reprogramming frequency.

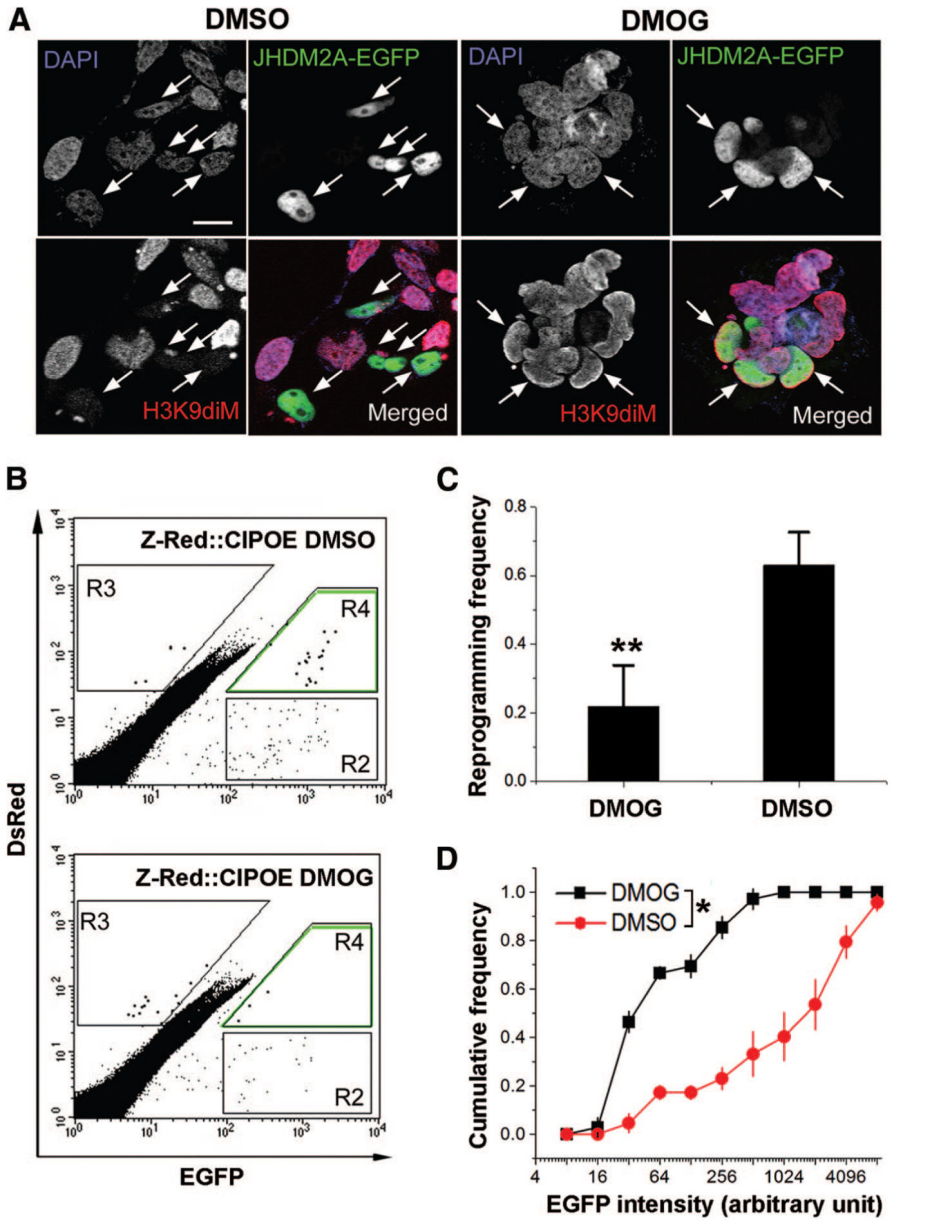

Figure 3.

Dioxygenase inhibitor DMOG impedes reprogramming. **(A):** Inhibition of Jhdm2a-induced histone demethylation by DMOG. Blocking effects of DMOG on Jhdm2a were examined in 293T cells transfected with a plasmid expressing the Jhdm2a-EGFP fusion protein. In control cells treated with DMSO, H3K9diM immunostaining signal was lost in Jhdm2a-EGFP transfected cells (arrows). With the treatment of 10 μM DMOG, H3K9diM signals were present in all cells regardless of Jhdm2a-EGFP expression. Scale bar = 20 μm. **(B–D):** DMOG attenuates ESC-induced reactivation of Oct4 expression from adult neural stem cells/progenitors. Polyethylene glycol-mediated cell fusion population treated with DMSO or DMOG (10 μM) was analyzed at day 4 and is displayed in dot plots. Representative plots from multiple experiments are shown **(B)**. Reprogramming frequencies from multiple

experiments were quantified **(C)** for fusion population with 48-hour treatment with DMSO or DMOG. Data represent mean ± SEM ($n = 3$; **, $p < .01$, Student's t test). Shown in **(D)** is the cumulative distribution plot of $DsRed^+$ population with graded EGFP fluorescence intensities for comparison of the reprogramming efficacy in the presence of DMSO or DMOG ($n = 3$ experiments; *, $p < .01$, Kolmogorov-Smirnov test). Abbreviations: DAPI, 4′, 6-diamidino-2-phenylindole; DMOG, dimethyloxalylglycine; DMSO, dimethyl sulfoxide; EGFP, enhanced green fluorescent protein; H3K9diM, histone H3 lysine 9 dimethylation.

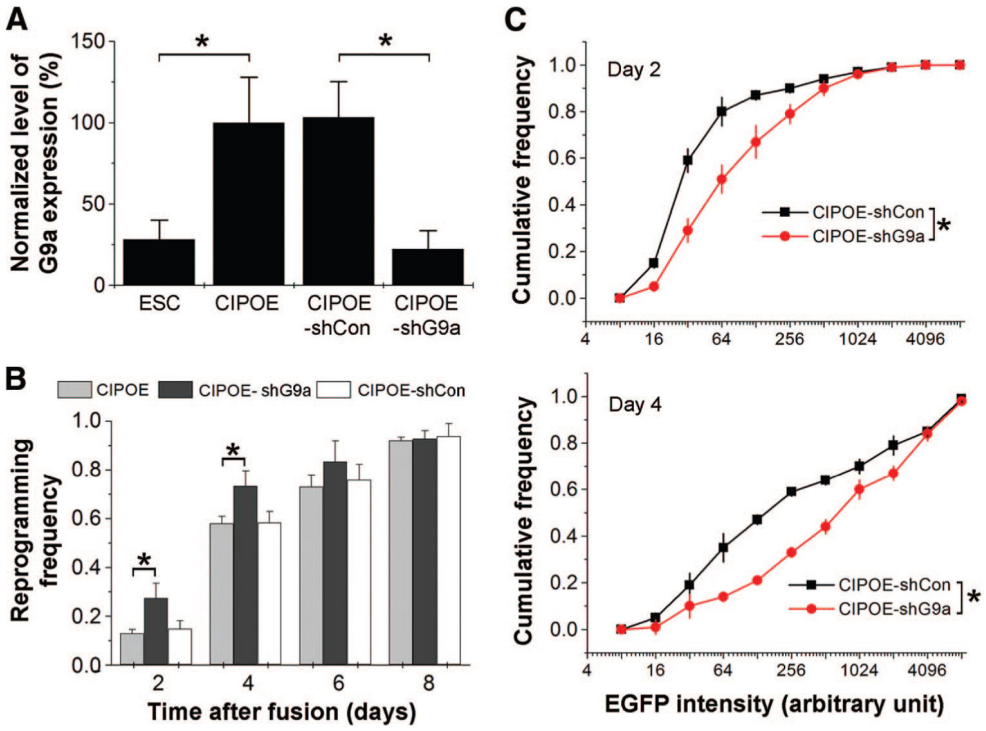

Figure 4.

Histone methyltransferase G9a restricts Oct4-EGFP reactivation during ESC-induced reprogramming. **(A):** Expression of G9a in ESCs and adult neural stem cells/progenitors (NSCs). Shown is a summary of quantitative real-time polymerase chain reaction analysis of the expression level of G9a in Z-Red ESCs, CIPOE NSCs, CIPOE NSCs with shCon, and shG9a. The mRNA abundance was normalized to the levels in CIPOE cells. Values represent mean ± SEM ($n = 3$; *, $p < .01$, Student's t test). **(B):** Summary of reprogramming frequencies. Shown are results from cell fusion experiments between Z-Red and CIPOE, CIPOE-shCon, or CIPOE-shG9a cells. Values represent mean ± SEM ($n = 3$; *, $p < .01$, Student's t test). **(C):** Summary of reprogramming efficacy. Cumulative distribution plots of $DsRed^+$ population with graded EGFP fluorescence intensities are shown for comparison of the reprogramming efficacy of Z-Red ESCs with CIPOE-shCon, or CIPOE-shG9a cells at days 2 and 4 after cell fusion. Values represent mean ± SEM ($n = 3$; *, $p < .01$, Kolmogorov-Smirnov test). Abbreviations: EGFP, enhanced green fluorescent protein; shCon, control short hairpin RNA; shG9a, G9a-targeted short hairpin RNA.

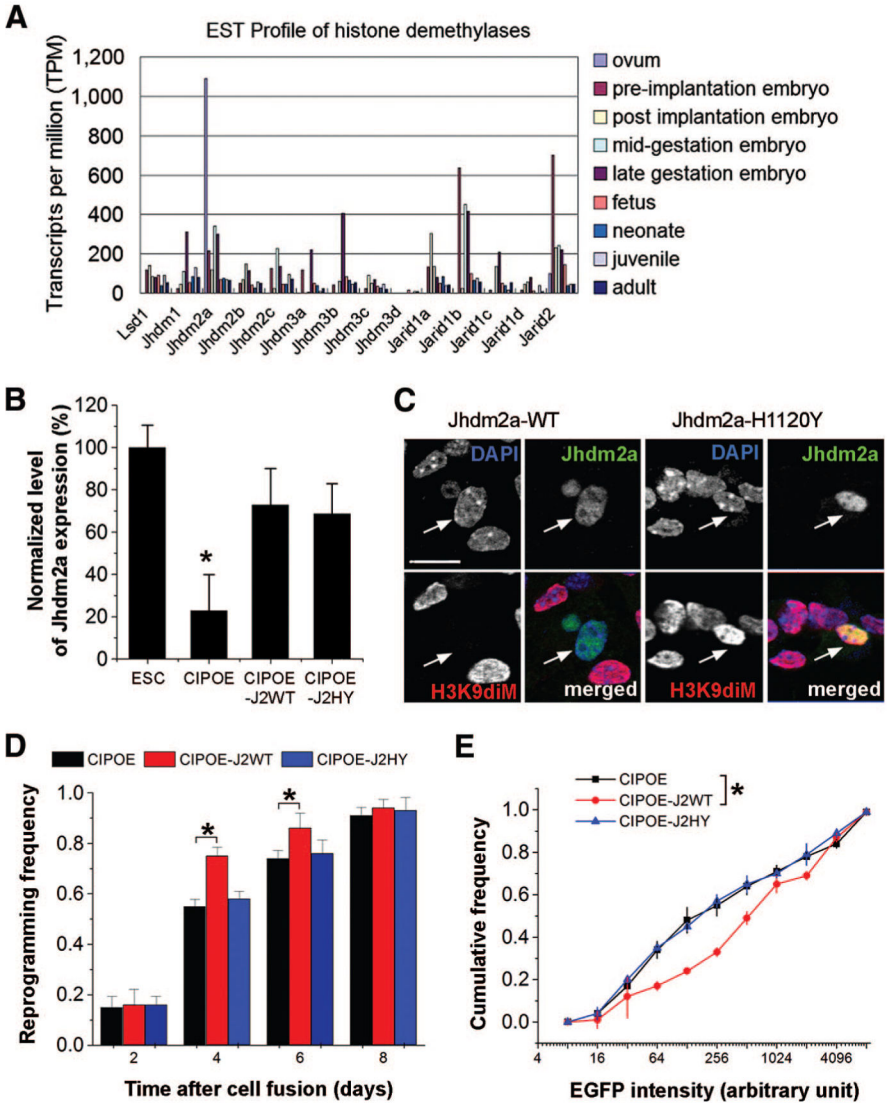

Figure 5.

Histone demethylase Jhdm2a facilitates Oct4 reactivation during ESC-induced reprogramming. **(A):** EST profiles of histone demethylases. EST counts (transcripts per million) were collected from National Center for Biotechnology Information Unigene expression resources (http://www.ncbi.nlm.nih.gov/sites/entrez) and plotted against a panel of currently identified histone demethylases. Distributions of EST for individual demethylases across different developmental stages are shown. **(B):** Expression of Jhdm2a in ESCs and adult neural stem cells/progenitors (NSCs). Shown are quantitative real-time polymerase chain reaction analyses of the expression levels of Jhdm2a in Z-Red ESCs, CIPOE NSCs, and CIPOE NSCs with virally transduced Jhdm2a WT or H1120Y enzymatically inactive mutant. mRNA abundance is normalized to the levels of Z-Red cells, and values represent mean ± SEM ($n = 3$; *, $p < .01$, Student's t test). **(C):** Ectopic expression of Jhdm2a, but not the enzyme-inactive mutant, induces global loss of H3K9 dimethylation in CIPOE NSCs, as indicated by arrows. Scale bar = 20 μm. **(D):** Summary of reprogramming frequencies. Shown are results from cell fusion experiments between Z-Red

and CIPOE, CIPOE-J2WT, or CIPOE-J2HY cells. Values represent mean ± SEM ($n = 3$; *, $p < .01$, Student's t test). **(E):** Summary of reprogramming efficacy. Cumulative distribution plots of $DsRed^+$ population with graded EGFP fluorescence intensities are shown for comparison of the reprogramming efficacy of Z-Red ESCs with CIPOE-J2 or CIPOE-J2HY cells at day 4 after cell fusion. Values represent mean ± SEM ($n = 3$; *, $p < .01$, Kolmogorov-Smirnov test). Abbreviations: DAPI, 4′,6-diamidino-2-phenylindole; EGFP, enhanced green fluorescent protein; EST, expressed sequence tag; H3K9diM, histone H3 lysine 9 dimethylation; TPM, transcripts per million; WT, wild-type.

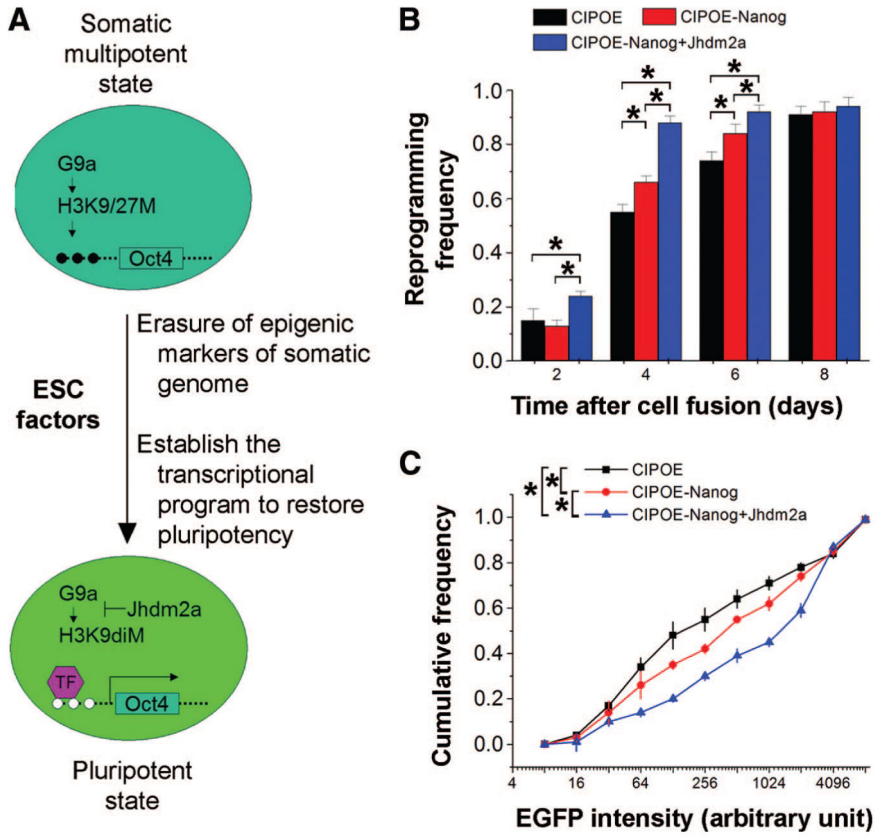

Figure 6.

Synergistic enhancement of reprogramming by a combination of Jhdm2a with the pluripotency-specific transcription factor Nanog. **(A):** A schematic drawing of the model on mechanisms underlying ESC fusion-induced Oct4-EGFP reactivation during reprogramming of somatic neural stem cells/progenitors. **(B):** Summary of reprogramming frequencies. Shown are results from cell fusion experiments between Z-Red and CIPOE, CIPOE-Nanog, or CIPOE-Nanog plus Jhdm2a cells. Values represent mean ± SEM ($n = 3$; *, $p < .01$, Student's t test). **(C):** Summary of reprogramming efficacy. Cumulative distribution plots of $DsRed^+$ population with graded EGFP fluorescence intensities are shown for comparison of the reprogramming efficacy of Z-Red ESCs with CIPOE, CIPOE-Jhdm2a, or CIPOE-Nanog plus Jhdm2a cells at day 4 after cell fusion. Values represent mean ± SEM ($n = 3$; *, $p < .01$, Kolmogorov-Smirnov test). Abbreviations: EGFP, enhanced green fluorescent protein; H3K9diM, histone H3 lysine 9 dimethylation.

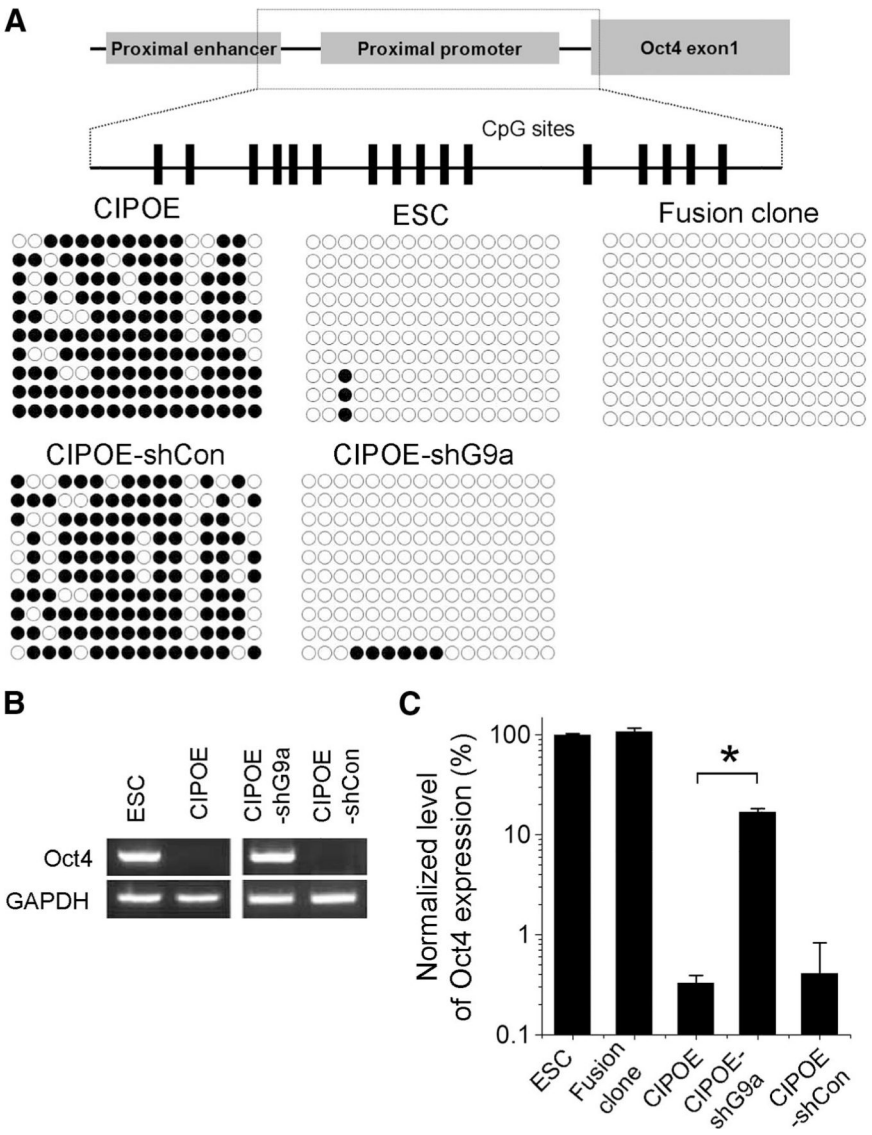

Figure 7.

Oct4 reactivation and promoter demethylation in adult neural stem cells/progenitors (NSCs) after G9a knockdown. **(A):** A schematic drawing of the Oct4 promoter with 16 CpG sites located between the proximal enhancer and exon 1. Bisulfite sequencing analysis was performed using genomic DNA extracted from CIPOE, Z-Red ESCs, fusion clone B3, CIPOE-shCon, and CIPOE-shG9a NSCs. **(B, C):** Conventional real-time polymerase chain reaction (PCR) **(B)** and quantitative real-time PCR **(C)** were used to compare the mRNA abundance of Oct4 in CIPOE, Z-Red ESCs, fusion clone B3, CIPOE-shCon, and CIPOE-shG9a NSCs. Data represent mean ± SEM ($n = 3$; *, $p < .01$, Student's t test). Abbreviations: GAPDH, glyceraldehyde-3-phosphate dehydrogenase; shCon, control short hairpin RNA; shG9a, G9a-targeted short hairpin RNA.